MOLECULAR AND CELLULAR BIOLOGY, June 2007, p. 4340–4346 Vol. 27, No. 12
0270-7306/07/$08.00+0 doi:10.1128/MCB.00379-07

N-Glycolylneuraminic Acid Deficiency in Mice: Implications for Human Biology and Evolution▽

Maria Hedlund,[1,6] Pam Tangvoranuntakul,[1,6] Hiromu Takematsu,[7,9] Jeffrey M. Long,[3] Gary D. Housley,[4] Yasunori Kozutsumi,[7,8,9] Akemi Suzuki,[8] Anthony Wynshaw-Boris,[1,3] Allen F. Ryan,[4,5] Richard L. Gallo,[1,3] Nissi Varki,[2] and Ajit Varki[1,6]*

Glycobiology Research and Training Center, Departments of Medicine,[1] Pathology,[2] Pediatrics,[3] Surgery,[4] Neurosciences,[5] and Cellular & Molecular Medicine,[6] University of California, San Diego, and VA Medical Center, La Jolla, California 92093-0687, and Laboratory of Membrane Biochemistry and Biophysics, Graduate School of Biostudies, Kyoto University, Kyoto,[7] Supra-biomolecular System Research Group, RIKEN Frontier Research System, Wako, Saitama,[8] and Core Research for Evolutional Science and Technology, Japan Science and Technology Agency, Kawaguchi,[9] Japan

Received 1 March 2007/Accepted 28 March 2007

Humans and chimpanzees share >99% identity in most proteins. One rare difference is a human-specific inactivating deletion in the *CMAH* gene, which determines biosynthesis of the sialic acid *N*-glycolylneuraminic acid (Neu5Gc). Since Neu5Gc is prominent on most chimpanzee cell surfaces, this mutation could have affected multiple systems. However, Neu5Gc is found in human cancers and fetuses and in trace amounts in normal human tissues, suggesting an alternate biosynthetic pathway. We inactivated the mouse *Cmah* gene and studied the in vivo consequences. There was no evidence for an alternate pathway in normal, fetal, or malignant tissue. Rather, null fetuses accumulated Neu5Gc from heterozygous mothers and dietary Neu5Gc was incorporated into oncogene-induced tumors. As with humans, there were accumulation of the precursor *N*-acetylneuraminic acid and increases in sialic acid O acetylation. Null mice showed other abnormalities reminiscent of the human condition. Adult mice showed a diminished acoustic startle response and required higher acoustic stimuli to increase responses above the baseline level. In this regard, histological abnormalities of the inner ear occurred in older mice, which had impaired hearing. Adult animals also showed delayed skin wound healing. Loss of Neu5Gc in hominid ancestors ~2 to 3 million years ago likely had immediate and long-term consequences for human biology.

Sialic acids (Sias) are nine-carbon sugars typically found at the terminal end of mammalian glycoconjugates, serving roles such as being receptors for pathogens or mediating cell-cell interactions or cell signaling by endogenous lectins. Since they are so widespread on all mammalian cell surfaces, alterations in the Sia repertoire could have diverse effects on multiple biological systems. The most common mammalian Sias are *N*-acetylneuraminic acid (Neu5Ac) and *N*-glycolylneuraminic acid (Neu5Gc). Neu5Gc is generated by hydroxylation of CMP-Neu5Ac to CMP-Neu5Gc, catalyzed by CMP-Neu5Ac hydroxylase (CMAH). Although abundant in many mammals, including the chimpanzee and other great apes (our closest evolutionary relatives), Neu5Gc is difficult to detect in humans (37). (The term "great apes" is used in the colloquial sense, since genomic information no longer supports this species grouping [13]. These species are now grouped with humans in the family *Hominidae*.) However, Neu5Gc was found in human tumors and fetal samples (11, 15, 16, 18, 24, 27, 37) and assumed to be an "oncofetal" antigen, i.e., the result of a gene being expressed in tumors and fetuses but not in adults. An exon deletion/frameshift mutation in the human *CMAH* gene was then discovered (7, 17, 37), indicating that the major pathway for Neu5Gc production in humans has been eliminated. However, the presence of Neu5Gc in human tumors was confirmed chemically (24), and we then found small amounts in some normal human tissues (36). Taken together, these data raised the possibility of an alternate biosynthetic pathway for Neu5Gc biosynthesis (24). However, existing biochemical pathways allow exogenous Neu5Gc to be metabolically incorporated into cultured human cells (3). We therefore suggested that Neu5Gc in normal human tissues, tumors, and fetuses originates with dietary sources (36), which include red meat and milk products. Genetic elimination of the single-copy *CMAH* gene in a model system can address this controversy. Given that *CMAH* is present only in the deuterostome lineage of animals (vertebrates and "higher" invertebrates) (31) and the ethical and practical limitations of primate studies, the logical candidate is the mouse.

Sias are also binding sites for many pathogens and toxins, and the single-oxygen-atom difference between Neu5Ac and Neu5Gc can affect these processes (25, 30, 32, 35). However, complete elimination of Sias is not an evolutionary option, since this causes embryonic lethality (33), likely because Sias are also important mediators of many intrinsic receptor-binding processes, such as those involving Siglecs (Sia-binding immunoglobulin superfamily lectins) (10, 39). Some Siglecs preferentially bind Neu5Ac-containing structures, e.g., myelin-associated glycoprotein (Siglec-4/MAG) on neuronal membranes, which stabilizes the axonal myelin sheath (8), and sialoadhesin

* Corresponding author. Mailing address: UCSD, 9500 Gilman Drive, MC 0687, La Jolla, CA 92093-0687. Phone: (858) 534-2214. Fax: (858) 534-5611. E-mail: a1varki@ucsd.edu.
▽ Published ahead of print on 9 April 2007.

on macrophages (5). These and other functions of Sias were likely altered by the loss of Neu5Gc production in the human lineage. We report an initial study of the consequences of inactivating the *Cmah* gene in mice, asking questions about the source of human "oncofetal" Neu5Gc, as well as some other features of the human condition. Rather than focusing on a single consequence of the mutation and analyzing it in detail, we report a variety of phenotypes arising from this human-like mutation in mice, some reminiscent of the human condition (20).

MATERIALS AND METHODS

Generation of targeting construct pFlox-Ex-SL for elimination of CMAH expression. A 10-kb genomic DNA region spanning the CMAH gene that includes the 92 bp corresponding to exon 6 of the murine *CMAH* gene was isolated from a bacterial artificial chromosome clone by digesting the clone with EcoRI, with subsequent Southern blotting using a radiolabeled probe corresponding to exon 6. The 10-kb piece was subcloned into pBluescript II KS(+), generating the construct pBS-35. Mapping of the restriction sites of the 10-kb fragment was performed by digesting pBS-35 with various restriction enzymes. A 535-bp fragment containing exon 6 was isolated from pBS-35 by digestion with NheI and XbaI and cloned into the BamHI site in the pFlox vector. A 1,150-bp intronic region directly upstream of the 535-bp fragment was isolated by digestion with NheI and subcloning into the pBluescript II KS(+) vector. This was then used for PCR using forward primer CGGCTCGAGTGAGCTACATGAGAT and reverse primer GGGCTCGAGTAATCACCAAGCAAA, thereby adding XhoI restriction sites to the ends of the 1,150-bp fragment. The PCR product was subcloned into the pBluescript II KS(+) vector, which was then digested with XhoI and cloned into the Xho site in the pFlox-Exon vector, creating the pFlox-Ex-S vector. Next, a 4,850-bp fragment directly downstream of the 535-bp fragment was excised from pBS-35 by digestion with XbaI and NheI and cloned into the XbaI site in the pFlox-Ex-S vector, generating the final targeting construct, pFlox-Ex-SL.

Generation of Cmah$^{-/-}$ mice. The pFlox-Ex-SL plasmid DNA was purified by a standard cesium chloride method and linearized by digestion with the restriction enzyme NotI. The solution containing digested plasmid DNA was then subjected to sequential phenol, 1:1 phenol:chloroform, and chloroform extraction. The aqueous phase containing the linearized DNA was then subjected to sodium acetate precipitation. The resulting DNA pellet was washed two times in ice-cold 70% ethanol, air dried, and resuspended in Tris-EDTA. The generation of the transgenic mice was performed by the University of California, San Diego (UCSD), Transgenic Mouse Core. In brief, the linearized transgenic constructs were electroporated into embryonic stem cells (ES cells) isolated from the 129/SvJ mouse strain. The ES cells then underwent drug selection, subclone isolation, and growth of isolated clones. Each clone was grown in triplicate plates, one that was kept by the Transgenic Mouse Core as a master plate that was frozen at −80°C and two that were returned to investigators for the identification of homologous recombinants. DNA was purified from each clone and subjected to screening by PCR and Southern blot analysis as described below. Homologous recombinants were thawed, expanded, and reconfirmed by PCR and Southern blot analysis. For the generation of the *Cmah*$^{-/-}$ mouse, homologous recombinant clones were subjected to transfection with a Cre recombinase expression vector, ganciclovir drug selection against the presence of thymidine kinase, subclone isolation, and growth of isolated clones. The desired type of recombination was then identified by PCR analysis. Karyotyping was then performed, and two of the best clones were selected for blastocyst injection. Chimeric mice were then generated and bred to C57Bl/6 females to allow germ line transmission of the transgene.

PCR genotyping analysis of *Cmah*$^{-/-}$ mice. To genotype the mice, DNA isolated from toe clips was used for PCR analysis. Toe clips performed to mark the identities of the mice were collected and digested in 20 μl of buffer containing 50 mM Tris, pH 8.0, 20 mM NaCl, 1 mM EDTA, 1% sodium dodecyl sulfate, and 250 μg/ml proteinase K at 55°C until the soft tissue dissolved. The sample was then diluted with 180 μl of water and boiled to inactivate the enzyme. For genotyping of *CMAH*$^{-/-}$ mice, PCR primers UpExon6 (CCAGGAGGAGTTA CCCTGAA) and DwExon6 (CGAGGACAGCCCAGAGACTA) were designed based on the published murine *CMAH* sequence. Analysis was performed using the following PCR cycle: 94°C for 5 min; 40 cycles of 94°C for 30 s, 53°C for 30 s, and 72°C for 1 min; and 72°C for 5 min. A PCR product of 305 bp was generated from the deletion allele, while a product of 490 bp is generated from the wild-type (WT) allele.

Animal care. All animals used were maintained in an access-controlled barrier facility under specific-pathogen-free conditions. Studies were performed in accordance with Public Health Service guidelines and approved by the Animal Subjects Committee of the University of California, San Diego. Animals were fed either a normal chow diet or a soy chow diet (AIN-93 M; Dyets, Bethlehem, PA).

DMB-HPLC analysis of Neu5Gc content in cells and tissues. Cells or tissues were homogenized and subjected to acid hydrolysis using 2 M acetic acid at 80°C for 3 h to release Sias from cellular glycoconjugates. After centrifugation at 20,000 × *g*, the supernatant was filtered through a Microcon 10 unit, dried down, and reconstituted in water. Aliquots were derivatized with 1,2-diamino-4,5-methylene dioxybenzene (DMB) and analyzed by high-performance liquid chromatography (HPLC). To remove base-labile *O*-acetyl esters, samples were first incubated with 0.1 M NaOH for 30 min at room temperature.

Immunohistochemistry. Tissues were frozen in optimal cutting temperature compound and archived at −70°C. Prior to staining, sections were air-dried for 30 min and fixed in 10% buffered formalin for 30 min, and endogenous peroxidase activity was quenched and nonspecific binding sites blocked with 5% human serum in phosphate-buffered saline (PBS) for 30 min. Sections were then incubated with the chicken anti-Neu5Gc antibody in 5% human serum–PBS at a 1:200 dilution at room temperature for 2 h. After washing, horseradish peroxidase-conjugated donkey anti-chicken immunoglobulin Y (IgY) antibody in PBS at a 1:100 dilution was applied for 1 h. Control sections were incubated with secondary reagent only or a control chicken IgY antibody. Specific binding was detected using the AEC substrate kit.

Behavioral and cognitive assessment of CMAH-deficient mice. Four separate groups of 7 to 10 null mice and WT controls were subjected the behavioral tests. The first cohort consisted of 4-month-old male mice ($n = 10$ *Cmah*$^{+/+}$ mice; $n = 10$ *Cmah*$^{-/-}$ mice) run in the entire battery. The second cohort consisted of 4-month-old male mice ($n = 10$ *Cmah*$^{+/+}$ mice; $n = 7$ *Cmah*$^{-/-}$ mice), which were subjected to the rotorod, open field, startle response, and prepulse inhibition (PPI) tests. The third cohort of 3-month-old male mice ($n = 10$ *Cmah*$^{+/+}$ mice; $n = 10$ *Cmah*$^{-/-}$ mice) was tested in the complete battery, and a forth cohort of 10-month-old mixed-sex mice ($n = 3$ male *Cmah*$^{+/+}$ mice; $n = 5$ female *Cmah*$^{+/+}$ mice; $n = 6$ male *Cmah*$^{-/-}$ mice; $n = 4$ female *Cmah*$^{-/-}$ mice) was subjected to the rotorod and threshold-to-startle response tests.

The test battery assessed mice on a variety of parameters, including gross physical assessment, sensorimotor reflexes, motor activity (initiation of movement, open field, wire hang, grip strength, cage top hang test, rotorod and pole test), nociception (hot plate and tail flick), acoustic startle, sensorimotor gating (PPI), and learning and memory (fear conditioning, passive avoidance, and water maze). The test battery was run as described previously (9, 23), with the exception of the rotorod test for the first cohort. Locomotor coordination and balance were measured by placing mice on an accelerating, 3-cm-diameter, rotating drum (UGO Basile, Varese, Italy) for three trials with a minimum 15-min interval between trials. The rotarod started with a rotating speed of 4 rpm and increased to 40 rpm over a 5-min period. The mean latency to fall over the three trials was recorded. For the first cohort of mice only, three additional days of testing (four trials per day) were administered to assess motor learning.

Studies of inner ear histology and ABR. For histology, inner ears were harvested after intracardiac perfusion with 4% paraformaldehyde, postfixed overnight, decalcified in 8% EDTA, and embedded in Araldite. Sections were stained with toluidine blue for light microscopy. To assess the auditory brainstem response (ABR), a loudspeaker was coupled to the ear of anesthetized mice and subcutaneous electrodes were inserted at the vertex and behind the pinna, with ground on a rear leg. ABRs were averaged over 512 trials using a Tucker-Davis Technology System III unit. Clicks and 25-ms tone bursts (4, 8, 12, 16, 24, and 32 kHz) were delivered at 20/s, starting at 90 dB and decreasing in 5-dB steps to reach threshold.

Wound healing assay. Murine cutaneous wound repair was evaluated as described previously (22). Sex- and age-matched adult mice were anesthetized by isoflurane inhalation and shaved, and hair was removed by chemical depilation (Nair). A single 4-mm wound was made with a dermal biopsy punch on the dorsal skin of each mouse. Daily measurements of the wound area were determined by using digital images of the wounds. The wound edge was defined on each digital image and the area of the enclosed wound site calculated directly using NIH image software. Experiments were done with humane care in compliance with institutional guidelines and with approval of the VA San Diego Healthcare System subcommittee on animal care, protocol no. 05-041.

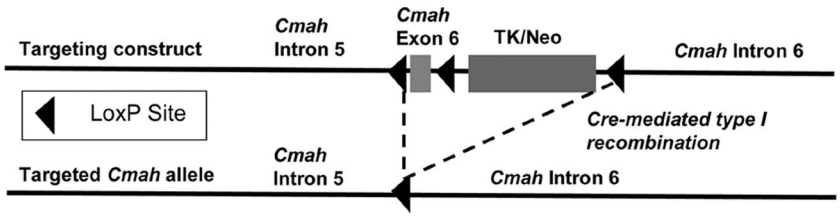

FIG. 1. Generation of the human-like *Cmah*$^{-/-}$ mouse. The targeting construct and final targeted *Cmah* allele are shown.

RESULTS AND DISCUSSION

Generation of Cmah null mice. Two laboratories independently produced *Cmah*$^{-/-}$ mice using different approaches, and most results are combined here for optimal presentation. One *Cmah*$^{-/-}$ strain was generated by Neo cassette insertional mutagenesis in mouse ES cells, which disrupted the reading frame of the *Cmah* gene, and a resulting mouse-specific B-cell defect not present in humans has been described elsewhere (28). The second ES-cell targeting caused a human-like deletion of exon 6 of the *Cmah* gene, using loxP sites and Cre recombinase expression in ES cells (Fig. 1). Both strains were viable and fertile under standard vivarium conditions and were fully backcrossed to a C57Bl/6 genetic background (>10 generations) prior to performing the studies reported here (unless otherwise stated, all studies were done at UCSD in compliance with institutional guidelines and with the approval of the IACUC). No obvious differences between the two strains were noted in any of the studies.

***CMAH* disruption causes complete deficiency in Neu5Gc expression.** An earlier screen of tissues from *Cmah*$^{-/-}$ mice with the Neo cassette insertion showed no detectable Neu5Gc using an HPLC method (<2% of total Sias) (28). Here we checked to see if even small traces are present, generated via any alternate pathway. Standard mouse chow contains significant amounts of Neu5Gc, presumably because of animal-based additives (detected by acid release, derivatization with DMB), and analysis by HPLC [DMB-HPLC]; data not shown). Null mice of both types were therefore weaned on a soy-based vegan diet confirmed to be free of Neu5Gc by DMB-HPLC (data not shown). Multiple tissues from such adult animals were analyzed for Neu5Gc expression by immunohistochemistry using a sensitive chicken polyclonal antibody specific for Neu5Gc (36). While WT mice showed complex staining patterns (Fig. 2A), there was no staining in most null tissues. The only exception was weak and variable staining in the mucinous secretions of the gut epithelium and pancreas (see Fig. 2A). To pursue this further, Sias in glycopeptides and lipid extracts were analyzed by DMB-HPLC. While WT mice showed easily detectable Neu5Gc in most tissues, none was detected in any tissues of the null animals, including the pancreas, the small intestine, and the colon (data not shown). Complete Neu5Gc absence was confirmed by mass spectrometric analysis of DMB-derivatized Sias (36) from these organs (data not shown). Thus, the weak antibody staining represents an artifact, likely caused by a high density of other Sia types in mucinous secretions of these organs.

We also did not see accumulation of Neu5Gc in tissues of

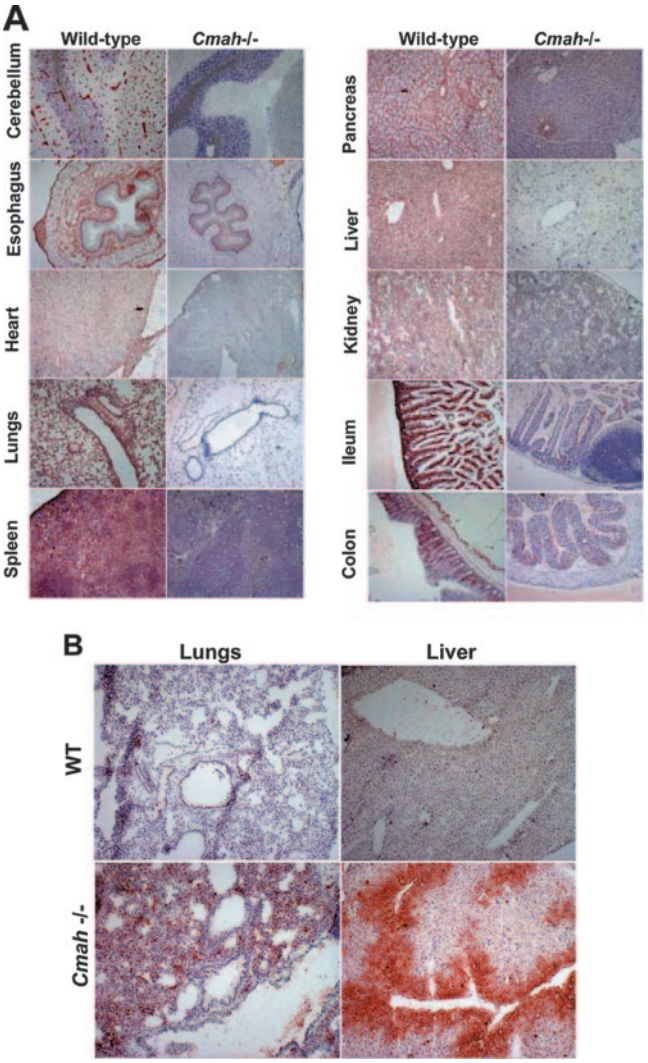

FIG. 2. *Cmah*$^{-/-}$ mice are deficient in Neu5Gc. (A) Neu5Gc expression was studied by immunohistochemistry in multiple tissues from multiple animals using a chicken anti-Neu5Gc antibody, and examples are shown. The few null tissues staining weakly positive were studied by acid hydrolysis, DMB-HPLC, and mass spectrometry analysis, showing no evidence of Neu5Gc. (B) Increased 9-O acetylation of Neu5Ac in *Cmah* null mice. The CHE-FcD probe was precomplexed with horseradish peroxidase-conjugated goat anti-human IgG at an optimized ratio and applied to sections of tissues from WT and *Cmah*$^{-/-}$ animals. Magnification, ×100. Brownish-red color represents positive staining.

TABLE 1. Sias of erythrocyte ghosts and plasma proteins of WT and *Cmah* null mice[a]

Genotype	Sample (n^b)	% of total Sias			
		Neu5Ac	O-acetylated Neu5Ac	Neu5Gc	O-acetylated Neu5Gc
WT	Ghosts (3)	49–59	23–36	7–18	<0.5
	Plasma (5)	18–25	1–4	71–81	<0.5
Cmah$^{-/-}$	Ghosts (3)	55–72	28–45	<0.5	<0.5
	Plasma (5)	85–90	10–15	<0.5	<0.5

[a] Plasma and erythrocyte ghosts were subjected to mild acid hydrolysis and the released Sias studied by DMB derivatization and HPLC as described in Materials and Methods. Most O-acetylated Sias had a single *O*-acetyl ester at the 7, 8, or 9 position, and these are quantitated together, since the esters can easily migrate from the 7 or 8 position to the 9 position.

[b] *n*, no. of samples.

null mice exposed to 1 mg/ml free Neu5Gc in their drinking water over several weeks (daily water consumption rates were not affected). Of course, our earlier human ingestion study (36) showed very little incorporation of a single large oral dose. Overall, we conclude that the small amounts of Neu5Gc found in normal human autopsy tissues are not generated by a second mammalian biosynthetic pathway but likely accumulates from dietary sources over many years.

Increased O acetylation of Sias. Another common modification of Sia is substitution of the 9-hydroxyl group with an *O*-acetyl ester. This modification can modulate recognition by intrinsic Sia binding molecules, such as Siglecs, as well as the various pathogen binding proteins (2, 19, 40). In a recent study, we noted increased O-acetylated Neu5Ac in human samples, compared with those of great apes (1). This difference could affect susceptibility to certain common cold viruses that selectively recognize O-acetylated Sias (40). Interestingly, the absence of Neu5Gc in the null animals results in increased 9-O acetylation of Neu5Ac in plasma and possibly erythrocytes (Table 1). Increased Sia 9-O acetylation was also found in some other tissues, such as liver and lung, by immunohistochemistry (Fig. 2B). Thus, these null mice mimic the human condition of relatively increased 9-O acetylation.

No alternative biosynthetic pathway for Neu5Gc in tumors or fetuses. We explored an alternative pathway for Neu5Gc expression as an oncofetal antigen, studying fetal development and spontaneously developing mammary tumors induced by a mouse mammary tumor virus-PyMT transgene (14). Fetuses and tumors from WT animals showed abundant expression of Neu5Gc (Fig. 3A and B, left panels). In contrast, *Cmah*$^{-/-}$ fetuses growing in null mothers revealed very weak reactivity within the basal layer of the epidermis, mucinous secretions of the small intestine, and the stomach (Fig. 3A, middle panel). There was no Neu5Gc detected in the embryos by the DMB-HPLC method, indicating that this is also nonspecific staining, as in the adult animals. Mammary tumors arising in null mice showed no detectable Neu5Gc (Fig. 3B, middle panel). Thus, there appears to be no alternative biosynthetic pathway for Neu5Gc production in mammalian tumor cells or fetuses.

Incorporation of exogenous Neu5Gc into fetuses and tumors of *Cmah* null mice. A *Cmah*$^{-/-}$ female mouse mated to a *Cmah*$^{-/-}$ male was fed with 1 mg/ml free Neu5Gc in drinking water from gestation day 13 through 18 and the fetuses analyzed for Neu5Gc expression. There was no definite change over the background level of staining seen in unfed animals (Fig. 3A, right panel), nor was there any chemical evidence of Neu5Gc incorporation, by DMB-HPLC analysis (not shown). Of course, this 5-day Neu5Gc feeding is short in comparison to the prolonged exposure of the human fetus to the maternal diet for >250 days. We therefore also studied *Cmah*$^{-/-}$ fetuses growing in a *Cmah*$^{+/-}$ female. In this case, all newborn pups showed strong anti-Neu5Gc antibody reactivity, even when they were genotypically *Cmah*$^{-/-}$ (Fig. 3C). Thus, *Cmah*$^{-/-}$ fetuses are capable of incorporation of Neu5Gc from maternal sources.

Although oral feeding did not cause Neu5Gc incorporation into adult or fetal mouse tissues, we did find incorporation into tumors. MMTV-PyMT transgenic *Cmah*$^{-/-}$ mice were fed with 1.5 mg of free Neu5Gc per ml in the drinking water for 1 month after onset of spontaneous mammary tumor growth. Positive staining with the anti-Neu5Gc antibody was detected

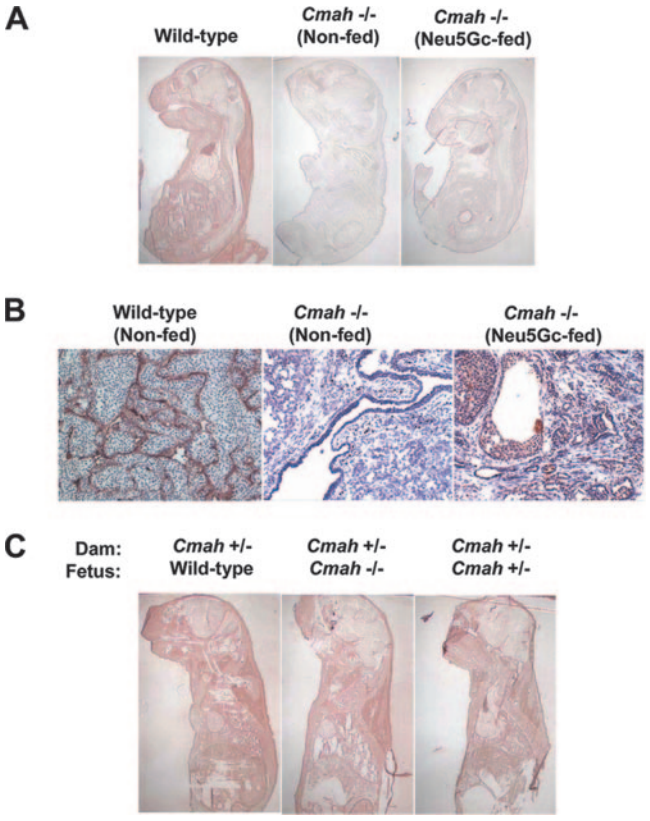

FIG. 3. No alternative pathway for Neu5Gc biosynthesis in fetuses or tumors. Neu5Gc expression was studied by immunohistochemistry as with Fig. 1. (A) Fetuses from *Cmah*$^{-/-}$ female mice with or without 1 mg/ml free Neu5Gc in the drinking water showed similar staining patterns with the anti-Neu5Gc antibody, indicating that reactivity is not due to uptake and incorporation. (B) *Cmah*$^{-/-}$ MMTV-PyMT transgenic mice were given Neu5Gc (1 mg/ml) free in the drinking water for 1 month after onset of mammary tumor growth. Positive staining for the anti-Neu5Gc antibody was detected, indicating that dietary Neu5Gc can be incorporated into tumors. Magnification, ×100. (C) A *Cmah*$^{+/-}$ female mouse was mated to a *Cmah*$^{+/-}$ male mouse. Pups were studied immediately after birth for Neu5Gc expression. Immunohistochemistry analysis of *Cmah*$^{+/+}$, *Cmah*$^{-/-}$, and *Cmah*$^{+/-}$ fetuses showed strong reactivity to all organs except for the brain.

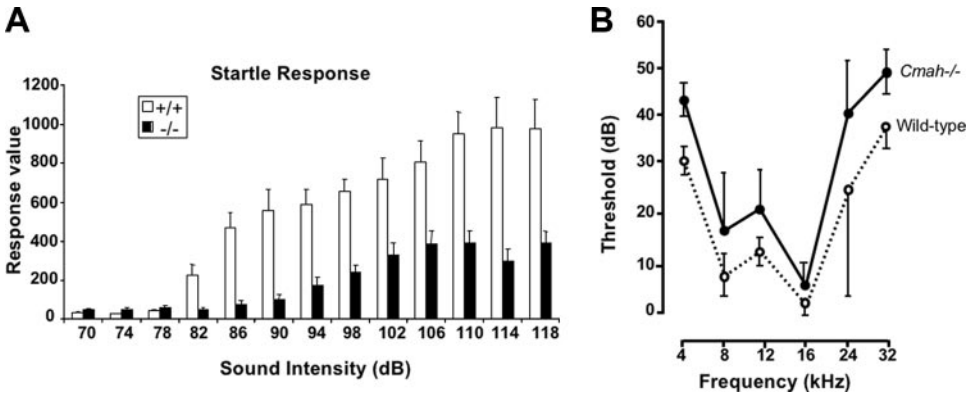

FIG. 4. Behavioral differences between *Cmah*$^{-/-}$ and WT mice. (A) Startle reflex differences represented by data from the fourth cohort. This result is representative of similar findings in three of four experiments. (B) ABR thresholds. A cohort of older (9 months) *Cmah*$^{-/-}$ mice had significantly reduced hearing sensitivity across the frequency range.

(Fig. 3B, right panel), albeit at levels lower than those seen in typical human tumors (36), which presumably accumulate exogenous Neu5Gc for much longer periods of time.

General behavioral and cognitive assessment. Expression of Neu5Gc in the mammalian brain is very low, even in species like the mouse and chimpanzee, in which expression in other tissues can be high (26, 29, 37). Here we show that this is true even in the fetal state (note the negative staining of the brain in the WT fetal sections in Fig. 3A and C). Meanwhile, the loss of Neu5Gc expression in the lineage leading to humans likely occurred ~2.5 to 3 million years ago (37), prior to the emergence of the genus *Homo*, an evolutionary stage associated with increasing brain size, tool use, and meat consumption via scavenging and/or hunting (6, 12, 41). We therefore carried out a general behavioral and cognitive assessment of *Cmah*$^{-/-}$ mice in comparison to WT controls. The test battery assessed mice on a variety of parameters (23). No statistically significant differences were observed in gross physical assessment, sensorimotor reflexes, nociception, and learning and memory in the two cohorts tested in the complete battery (data not shown). In the first cohort, *Cmah*$^{-/-}$ mice had impaired motor coordination as measured by the rotorod test (in both 1- and 3-day protocol), increased vertical activity in the open field test, and an abnormal startle response to acoustic stimuli and abnormal sensorimotor gating in the PPI task (data not shown). The second cohort was tested in these four assays (rotorod, open field, startle response, and PPI), with significant differences being replicated for the startle response and PPI test. PPI differences were also observed in the third cohort. Examination of the PPI data revealed that *Cmah*$^{-/-}$ mice were highly active in the restraint chamber (data not shown), and this increased the variability of the PPI measure to such an extent that an interpretation of the sensorimotor gating ability of the mice was impossible. Again, *Cmah*$^{-/-}$ mice were more active, possibly as a result of age-related changes in the inner ear (see below). *Cmah*$^{-/-}$ mice required higher acoustic stimuli to increase their startle response, a finding for three of four cohorts. An example shown in Fig. 4A demonstrates that *Cmah*$^{+/+}$ mice startle significantly above the 70-dB background level at a stimulus of 82 dB ($P < 0.05$), whereas *Cmah*$^{-/-}$ mice do not startle above the background level until 98 dB ($P < 0.05$). In addition, *Cmah*$^{-/-}$ mice showed a significantly lower ($P < 0.05$) startle response to acoustic startle stimuli between 82 and 118 dB (Fig. 4A). The potential hearing difficulties in the *Cmah*$^{-/-}$ mice found in three of the four cohorts prompted further investigations into the ABR threshold and inner ear morphology.

Disturbed hearing and inner ear histology. While 3-month-old *Cmah*$^{-/-}$ mice exhibited normal ABR thresholds, a cohort of 9-month-old mice had significantly reduced hearing sensitivity across frequencies (Fig. 4B). Nine-month- but not 3-month-old mice had abnormalities in the sensory epithelia of both the vestibular and auditory inner ears (Fig. 5). Unusual deposits of apparently acellular material were present on the apical surface of the vestibular otoconial epithelia, among the stereociliary bundles (Fig. 5A). This material could potentially affect the function of the stereocilia through mechanical interference. Alternatively, the material could reflect abnormal processes in the epithelium that decrease hair cell function. The semicircular canal organs showed a similar abnormality, although more subtly. In one null animal, a fluid-filled cyst was observed on a canal organ (Fig. 5C). In the cochlea, some 9-month-old mice showed outer hair cell degeneration throughout the cochlea, with collapse of the outer organ of Corti in the basal (high-frequency) turn (Fig. 5B). In contrast, both the cochlear and vestibular sensory epithelia of WT mice appeared normal, even in older animals.

Age-related hearing loss is common in humans, but unlike the flat loss seen in older *Cmah*$^{-/-}$ mice, human hearing loss is more prominent at high frequencies. There are many forms of age-related hearing loss in humans, due to damage to hair cells, neurons, secretory epithelia, etc. The *Cmah*$^{-/-}$ phenotype may be more similar to forms of late-onset deafness associated with hair cell loss. Though not precisely documented in the published literature, it is well accepted that humans have poorer hearing than most other mammals. In the only published study comparing chimpanzees with humans, the former were reported to be more sensitive than humans to frequencies above 8 kHz but less sensitive to 250-Hz and 2- to 4-kHz frequencies. Frequency and intensity difference thresholds are also greater for chimpanzees (21). Of course, since the *CMAH* mutation in humans occurred ~3 million year ago, the current

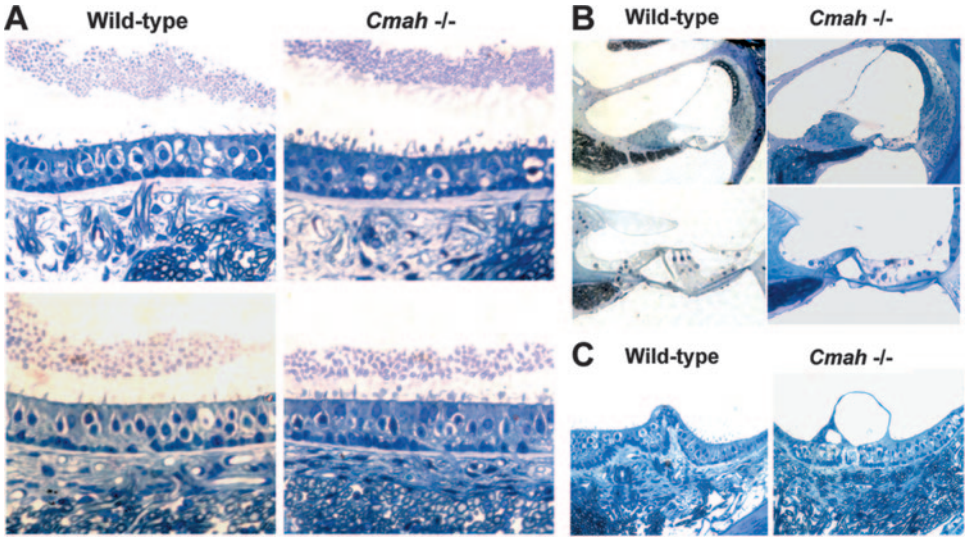

FIG. 5. Histological abnormalities in inner ears. (A) In the vestibular otoconial epithelia, unusual deposits of apparently acellular material were present on the apical surface of the epithelium, among the stereociliary bundles. (B) In the cochlear sensory epithelium, the area of the outer hair cells showed degeneration of the sensory cells throughout the cochlea, with collapse of the outer portion of the organ of Corti in the basal (high-frequency) turn. (C) Fluid-filled cyst observed on a semicircular canal organ of a null animal.

human condition likely represents a state of adaptation to any original changes. It also remains to be seen if the inconsistently reproducible balance problems seen in rotarod tests are also due to variable inner ear dysfunction. It is interesting to note that the emergence of the genus *Homo* seems to coincide with a shift from a mixed arboreal (climbing) and terrestrial (walking) behavior to a primarily terrestrial lifestyle, associated with the emergence of striding bipedal running (4, 20). A mild deterioration of balance in early *Homo* could have forced these adaptations.

Defects in wound healing. Strong anecdotal evidence indicates that nonhuman primates heal wounds faster than humans (34), and it is commonly known that chimpanzees "heal overnight," both in captivity (Jo Fritz, Primate Foundation of Arizona, personal communication) and in the wild (Pascal Gagneux, personal communication). The rates of induced wound healing in WT and null mice were therefore determined by daily measurements of the wound area. Wound repair was markedly delayed in the null animals, manifested most obviously as a decreased rate of closure between days 4 and 9 after injury (Fig. 6). Histological examination of wounds in this period revealed no obvious differences in inflammatory cell infiltrate, angiogenesis, or keratinocyte morphology. Further studies are needed to explore the molecular and cellular basis of this difference.

Conclusions and perspectives. We show here that the human-specific deletion in the *CMAH* gene very likely resulted in complete loss of Neu5Gc expression in all tissues. Thus, the frequent observation of Neu5Gc in human cancers and fetal tissues is not likely to be due to an alternate "oncofetal" metabolic pathway. Rather, the data support our hypothesis that the "oncofetal" expression of Neu5Gc (as well as the traces found in normal human tissues) likely originates with exogenous dietary sources. In support of this, free Neu5Gc can enter human cells via macropinocytosis to reach the endosomal/lysosomal system (3). There it can be transported into the cytosolic compartment and get activated to CMP-Neu5Gc, which would eventually enter the Golgi apparatus, where sialyltransferases can catalyze transfer of Neu5Gc to newly synthesized glycoconjugates. We have also shown that intact humans absorb a portion of ingested Neu5Gc, excrete it into the urine, and incorporate a small amount into newly synthesized glycoconjugates (36). The more prominent enrichment of Neu5Gc in carcinomas and fetuses could be due to a higher uptake by these rapidly growing tissues, perhaps associated with increased macropinocytosis induced by growth factors. Furthermore, hypoxic conditions in tumors have recently been shown to upregulate expression of the relevant lysosomal Sia transporter (42).

Since Neu5Gc is found in most cell types of great apes, the biological effects of its genetic loss in the human lineage are likely to be complex and/or variable. Of course, mice are not great apes, and we cannot expect that mice with a human-like deficiency of Neu5Gc will mimic all consequences of Neu5Gc

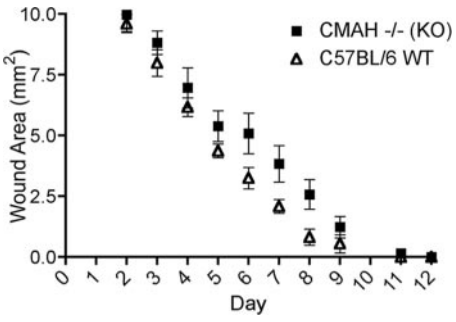

FIG. 6. Differences in cutaneous wound repair. A single wound was made with a dermal biopsy punch on the dorsal skin and measurements of wound area done by taking daily digital images. Data represent one experiment, with significance by one-way analysis of variance of a P value of <0.0001, seven mice per group, and are representative of similar findings in three experiments.

loss in a hominid ancestor. Furthermore, >2 million years have passed since the *CMAH* inactivation, and the current human condition likely represents a state of at least partial adaptation. Realizing these limitations, we have carried out an initial survey of some phenotypic features of these mice, finding subtle but significant differences reminiscent of the human condition, such as slowed wound healing and age-related hearing loss. Many additional studies will be needed to pursue these and other phenotypic features resulting from this human-like genetic defect. More ethically acceptable studies comparing the phenotypes of humans and great apes are also needed, since our knowledge of the great ape "phenome" (defined as "the body of information describing an organism's phenotypes, under the influences of genetic and environmental factors") (38) is currently quite limited.

ACKNOWLEDGMENTS

This work was supported by NIH grants HL057345 and GM32373 (to A.V.), the Mathers Foundation of New York, a postdoctoral fellowship from the STINT foundation (to M.H.), and grant DC00139 from the NIH/NIDCD and the Research Service of the VA (to A.F.R.).

REFERENCES

1. **Altheide, T. K., T. Hayakawa, T. S. Mikkelsen, S. Diaz, N. Varki, and A. Varki.** 2006. System-wide genomic and biochemical comparisons of sialic acid biology among primates and rodents: evidence for two modes of rapid evolution. J. Biol. Chem. **281:**25689–25702.
2. **Angata, T., and A. Varki.** 2002. Chemical diversity in the sialic acids and related alpha-keto acids: an evolutionary perspective. Chem. Rev. **102:**439–470.
3. **Bardor, M., D. H. Nguyen, S. Diaz, and A. Varki.** 2005. Mechanism of uptake and incorporation of the non-human sialic acid N-glycolylneuraminic acid into human cells. J. Biol. Chem. **280:**4228–4237.
4. **Bramble, D. M., and D. E. Lieberman.** 2004. Endurance running and the evolution of Homo. Nature **432:**345–352.
5. **Brinkman-Van der Linden, E. C. M., and A. Varki.** 2000. New aspects of siglec binding specificities, including the significance of fucosylation and of the sialyl-Tn epitope. J. Biol. Chem. **275:**8625–8632.
6. **Cela-Conde, C. J., and F. J. Ayala.** 2003. Genera of the human lineage. Proc. Natl. Acad. Sci. USA. **100:**7684–7689.
7. **Chou, H. H., H. Takematsu, S. Diaz, J. Iber, E. Nickerson, K. L. Wright, E. A. Muchmore, D. L. Nelson, S. T. Warren, and A. Varki.** 1998. A mutation in human CMP-sialic acid hydroxylase occurred after the Homo-Pan divergence. Proc. Natl. Acad. Sci. USA **95:**11751–11756.
8. **Collins, B. E., T. J. Fralich, S. Itonori, Y. Ichikawa, and R. L. Schnaar.** 2000. Conversion of cellular sialic acid expression from N-acetyl- to N-glycolylneuraminic acid using a synthetic precursor, N-glycolylmannosamine pentaacetate: inhibition of myelin-associated glycoprotein binding to neural cells. Glycobiology **10:**11–20.
9. **Corbo, J. C., T. A. Deuel, J. M. Long, P. LaPorte, E. Tsai, A. Wynshaw-Boris, and C. A. Walsh.** 2002. Doublecortin is required in mice for lamination of the hippocampus but not the neocortex. J. Neurosci. **22:**7548–7557.
10. **Crocker, P. R.** 2005. Siglecs in innate immunity. Curr. Opin. Pharmacol. **5:**431–437.
11. **Devine, P. L., B. A. Clark, G. W. Birrell, G. T. Layton, B. G. Ward, P. F. Alewood, and I. F. C. McKenzie.** 1991. The breast tumor-associated epitope defined by monoclonal antibody 3E1.2 is an O-linked mucin carbohydrate containing N-glycolylneuraminic acid. Cancer Res. **51:**5826–5836.
12. **Finch, C. E., and C. B. Stanford.** 2004. Meat-adaptive genes and the evolution of slower aging in humans. Q. Rev. Biol. **79:**3–50.
13. **Goodman, M.** 1999. The genomic record of humankind's evolutionary roots. Am. J. Hum. Genet. **64:**31–39.
14. **Guy, C. T., R. D. Cardiff, and W. J. Muller.** 1992. Induction of mammary tumors by expression of polyomavirus middle T oncogene: a transgenic mouse model for metastatic disease. Mol. Cell. Biol. **12:**954–961.
15. **Higashi, H., Y. Hirabayashi, Y. Fukui, M. Naiki, M. Matsumoto, S. Ueda, and S. Kato.** 1985. Characterization of N-glycolylneuraminic acid-containing gangliosides as tumor-associated Hanganutziu-Deicher antigen in human colon cancer. Cancer Res. **45:**3796–3802.
16. **Hirabayashi, Y., H. Higashi, S. Kato, M. Taniguchi, and M. Matsumoto.** 1987. Occurrence of tumor-associated ganglioside antigens with Hanganutziu-Deicher antigenic activity on human melanomas. Jpn. J. Cancer Res. **78:**614–620.
17. **Irie, A., S. Koyama, Y. Kozutsumi, T. Kawasaki, and A. Suzuki.** 1998. The molecular basis for the absence of N-glycolylneuraminic acid in humans. J. Biol. Chem. **273:**15866–15871.
18. **Kawachi, S., T. Saida, H. Uhara, K. Uemura, T. Taketomi, and K. Kano.** 1988. Heterophile Hanganutziu-Deicher antigen in ganglioside fractions of human melanoma tissues. Int. Arch. Allergy Appl. Immunol. **85:**381–383.
19. **Kelm, S., and R. Schauer.** 1997. Sialic acids in molecular and cellular interactions. Int. Rev. Cytol. **175:**137–240.
20. **Klein, R. G.** 1999. The human career: human biological and cultural origins. The University of Chicago, Chicago, IL.
21. **Kojima, S.** 1990. Comparison of auditory functions in the chimpanzee and human. Folia Primatol. (Basel) **55:**62–72.
22. **Lee, P. H., J. A. Rudisill, K. H. Lin, L. Zhang, S. M. Harris, T. J. Falla, and R. L. Gallo.** 2004. HB-107, a nonbacteriostatic fragment of the antimicrobial peptide cecropin B, accelerates murine wound repair. Wound Repair Regen. **12:**351–358.
23. **Long, J. M., P. Laporte, S. Merscher, B. Funke, B. Saint-Jore, A. Puech, R. Kucherlapati, B. E. Morrow, A. I. Skoultchi, and A. Wynshaw-Boris.** 2006. Behavior of mice with mutations in the conserved region deleted in velocardiofacial/DiGeorge syndrome. Neurogenetics **7:**247–257.
24. **Malykh, Y. N., R. Schauer, and L. Shaw.** 2001. N-glycolylneuraminic acid in human tumours. Biochimie **83:**623–634.
25. **Martin, M. J., J. C. Rayner, P. Gagneux, J. W. Barnwell, and A. Varki.** 2005. Evolution of human-chimpanzee differences in malaria susceptibility: relationship to human genetic loss of N-glycolylneuraminic acid. Proc. Natl. Acad. Sci. USA **102:**12819–12824.
26. **Mikami, T., M. Kashiwagi, K. Tsuchihashi, T. Daino, T. Akino, and S. Gasa.** 1998. Further characterization of equine brain gangliosides: the presence of GM3 having N-glycolyl neuraminic acid in the central nervous system. J. Biochem. (Tokyo) **123:**487–491.
27. **Miyoshi, I., H. Higashi, Y. Hirabayashi, S. Kato, and M. Naiki.** 1986. Detection of 4-O-acetyl-N-glycolylneuraminyl lactosylceramide as one of tumor-associated antigens in human colon cancer tissues by specific antibody. Mol. Immunol. **23:**631–638.
28. **Naito, Y., H. Takematsu, S. Koyama, S. Miyake, H. Yamamoto, R. Fujinawa, M. Sugai, Y. Okuno, G. Tsujimoto, T. Yamaji, Y. Hashimoto, S. Itohara, T. Kawasaki, A. Suzuki, and Y. Kozutsumi.** 2007. Germinal center marker GL7 probes activation-dependent repression of *N*-glycolylneuraminic acid, a sialic acid species involved in the negative modulation of B-cell activation. Mol. Cell. Biol. **27:**3008–3022.
29. **Nakao, T., K. Kon, S. Ando, and Y. Hirabayashi.** 1991. A NeuGc-containing trisialoganglioside of bovine brain. Biochim. Biophys. Acta **1086:**305–309.
30. **Ono, E., K. Abe, M. Nakazawa, and M. Naiki.** 1989. Ganglioside epitope recognized by K99 fimbriae from enterotoxigenic *Escherichia coli*. Infect. Immun. **57:**907–911.
31. **Schmidt, C. L., and L. Shaw.** 2001. A comprehensive phylogenetic analysis of Rieske and Rieske-type iron-sulphur proteins. J. Bioenerg. Biomembr. **33:**9–26.
32. **Schultze, B., C. Krempl, M. L. Ballesteros, L. Shaw, R. Schauer, L. Enjuanes, and G. Herrler.** 1996. Transmissible gastroenteritis coronavirus, but not the related porcine respiratory coronavirus, has a sialic acid (*N*-glycolylneuraminic acid) binding activity. J. Virol. **70:**5634–5637.
33. **Schwarzkopf, M., K. P. Knobeloch, E. Rohde, S. Hinderlich, N. Wiechens, L. Lucka, I. Horak, W. Reutter, and R. Horstkorte.** 2002. Sialylation is essential for early development in mice. Proc. Natl. Acad. Sci. USA **99:**5267–5270.
34. **Sullivan, T. P., W. H. Eaglstein, S. C. Davis, and P. Mertz.** 2001. The pig as a model for human wound healing. Wound Repair Regen. **9:**66–76.
35. **Suzuki, Y.** 2005. Sialobiology of influenza: molecular mechanism of host range variation of influenza viruses. Biol. Pharm. Bull. **28:**399–408.
36. **Tangvoranuntakul, P., P. Gagneux, S. Diaz, M. Bardor, N. Varki, A. Varki, and E. Muchmore.** 2003. Human uptake and incorporation of an immunogenic nonhuman dietary sialic acid. Proc. Natl. Acad. Sci. USA **100:**12045–12050.
37. **Varki, A.** 2001. Loss of N-glycolylneuraminic acid in humans: mechanisms, consequences and implications for hominid evolution. Am. J. Phys. Anthropol. Suppl. **33:**54–69.
38. **Varki, A., and T. K. Altheide.** 2005. Comparing the human and chimpanzee genomes: searching for needles in a haystack. Genome Res. **15:**1746–1758.
39. **Varki, A., and T. Angata.** 2006. Siglecs—the major subfamily of I-type lectins. Glycobiology **16:**1R–27R.
40. **Vlasak, R., W. Luytjes, W. Spaan, and P. Palese.** 1988. Human and bovine coronaviruses recognize sialic acid-containing receptors similar to those of influenza C viruses. Proc. Natl. Acad. Sci. USA **85:**4526–4529.
41. **Wood, B., and M. Collard.** 1999. Anthropology—the human genus. Science **284:**65–66.
42. **Yin, J., A. Hashimoto, M. Izawa, K. Miyazaki, G. Y. Chen, H. Takematsu, Y. Kozutsumi, A. Suzuki, K. Furuhata, F. L. Cheng, C. H. Lin, C. Sato, K. Kitajima, and R. Kannagi.** 2006. Hypoxic culture induces expression of sialin, a sialic acid transporter, and cancer-associated gangliosides containing non-human sialic acid on human cancer cells. Cancer Res. **66:**2937–2945.